

**Long-Term Seafloor Measurements of Water Pressure:
Normal Modes and Infragravity Waves**

Jean H. Filloux and Douglas S. Luther

*Scripps Institution of Oceanography
La Jolla, CA, 92093-0230, USA*

Alan D. Chave

*AT&T Bell Laboratories, Physics Research Branch
600 Mountain Ave., Murray Hill, NJ, 07974, USA*

XXth General Assembly, IUGG, Vienna, Austria, 11-24 August, 1991

Abstract

Highly precise measurements of water pressure, sampled every 2 minutes, were obtained with Bourdon tube sensors at the seafloor of the North Pacific during the 11-month Barotropic, ElectroMagnetic and Pressure EXperiment (BEMPEX). Five pressure records, separated by up to 1100 km, reveal a field of pressure that is remarkably uniform at all periods despite abrupt topography within the array. At periods $T > 1.7$ days, quasi-geostrophic dynamics predominates and direct atmospheric forcing is demonstrated with cross-spectral statistics; these results are discussed in the nearby poster by *Luther, Chave and Filloux*. At $T < 1.7$ days, gravity wave dynamics predominates. While no direct cross-spectral link with any atmospheric variable has yet been found at these shorter periods, the strong similarity of power spectral magnitudes and slopes between seafloor pressure and non-local surface air pressure seems unlikely to be coincidental.

High coherence is found among the pressure records at almost all periods, even for the largest separation of 1100 km. For the infragravity wave band (15 minutes $> T > 2$ minutes), a seasonally-dependent source in the vicinity of Vancouver Is., British Columbia, Canada, dominates the records, in agreement with a recent study by *Webb et al.* [1991] showing that coastal, rather than open ocean, sources dominate the deep ocean infragravity wave field. At periods of 15 minutes to 2 hours, coherence phases among the 5 pressure records cluster either around 0° or 180° , depending on the period and the distance between stations. These observations are interpreted as evidence for the existence of horizontally-standing gravity oscillations. Unlike the infragravity wave band, the power in the 15 minute to 2 hour band shows no seasonal variability.

Overview of the Experiment

BEMPEX was principally designed to ascertain the extent to which sub-inertial oscillations of pelagic barotropic currents are directly related to surface atmospheric forcing, to determine the dominant horizontal scales of these motions and to relate these motions to simple linear theories of free and forced sub-inertial oscillations at mid-latitudes. [A nearby poster by *Luther, Chave and Filloux* discusses the results from BEMPEX pertaining to these principal goals.] It is well known that bottom pressure in the deep ocean is dominated by non-baroclinic phenomena, so it was natural that BEMPEX should contain a suite of pressure instruments. This led to the development of a number of secondary experimental goals concerned with the exploration of the fluctuations of bottom pressure at super-inertial frequencies where few long-term, large-scale-array measurements have been made. Some of the results of this exploration are described in this poster.

BEMPEX lasted for about 11 months from August 1986 to June 1987. The array of seafloor pressure gauges, horizontal electrometers and three-component magnetometers was centered north of the Hawaiian Islands at approximately 40.5°N , 163°W . The array is overlaid in **FIGURE 1** on a map of the local topography. Those instruments with labels beginning with P are the pressure gauges. Of the six pressure instruments shown, all returned complete datasets except PL which had only a two-month record. The pressure gauge array spans 750 km N-S and 1100 km E-W. The topography of the region generally consists of low abyssal hills with a few seamounts and two fracture zones. The Mendocino F.Z. running through the southern portion of the array has the most substantial topography. Note that the right-hatched areas are deeper than 6000 m and the left-hatched areas are shallower than 5000 m.

Description of the Pressure Gauge

The pressure instruments are self-contained (**FIGURE 2**) and free-falling with timed releases in BEMPEX (current versions employ acoustic releases). The transducer is a multi-turn Bourdon tube with frictionless electro-optical readout [Filloux, 1969, 1970, 1980]. The design achieves a large dynamic range and exceptional sensitivity (typical least count of .02 mb), the latter due to a high-resolution optical angular detector. The instruments sampled pressure 32 times per hour, except for PK which sampled 64 times per hour.

Like most pressure gauges, this instrument suffers from a plastic creep due to the stress of abyssal pressures. However, the creep of the heat-treated ferro-nickel alloy (Ni Span C), out of which the Bourdon tube is constructed, is very well understood. The observed creep can be characterized by a simple, analytically-generated, monotonic and inherently smooth function of time, composed primarily of a power law in time whose coefficients are estimated by least squares. Removal of this estimated creep function from the observations may remove some 'real' information, but only at the very longest periods; for instance, amplitudes of oscillations at periods equal to or shorter than the record length are only trivially affected by the creep correction. During BEMPEX, the creep at each instrument was approximately 50 cm over the 11-month record length.

The pressure sensor is relatively insensitive to temperature as well as to temperature transients, although this feature is not needed in the nearly isothermal deep North Pacific. Pressure-signal calibration is frozen within quantities inherently unchangeable such as focal length of a lens, elastic constant of a Bourdon tube, magnetic moment of a small magnet, and number of turns of the Bourdon helix.

Auto-Spectra

The energy density spectra of the 5 complete bottom pressure records from BEMPEX are shown in **FIGURE 3**. Frequency-band averaging has been allowed to increase with frequency, accounting for the decreasing confidence interval width indicated by the distance between the converging and straight lines at the bottom of the figure. Every other point plotted is independent. The straight line with a ω^{-2} slope is a visual aid, while the line with a ω^{-1} slope is the estimated instrumental noise level [Filloux, 1980]. The records are each 7700 hours long.

The spectra reveal a field of bottom pressure that is remarkably uniform at all frequencies despite a maximum separation of 1100 km and despite the presence of significant topography within the array. Even at these deep ocean sites, nonlinear overtides (only the 8-hour tidal peak has a significant linear component) are readily apparent.

At short periods (2-10 minutes), the spectra are enhanced due to the presence of long-wavelength surface gravity waves that are directly wind-generated. [Note that instrument PK has a Nyquist period of 1.875 minutes, half the Nyquist period of the other instruments.] The humped shape of the spectrum at these short periods has been explained [Filloux, 1980] as due to the greater vertical attenuation of gravity waves as period decreases, combined with a decrease in the energy spectrum of these directly-forced waves as period increases. Coherence phases discussed later confirm the hypothesis that this infragravity wave band is dominated by propagating waves. The rms amplitude of oscillations in the 2-10 minute band is just under 0.1 mb.

Comparative Spectra

It is instructive to compare the BEMPEX bottom pressure spectra with nearby island sea level and air pressure spectra. The nearest island to the BEMPEX site is Midway at approximately 28°N, 177°W. **FIGURE 4** compares the pressure spectrum from PC (~ 41°N, 169°W) with a sub-surface pressure (SSP) spectrum from Midway (data collected during 1955), where SSP is sea level (converted to units of pressure under the hydrostatic approximation) plus air pressure. The spectra are quite dissimilar in energy levels and slopes, and they emphasize, at least, the high background energy levels (either due to instrumental noise or 'real' phenomena such as resonant trapped waves) at the island station at periods shorter than 1 day.

FIGURE 5 displays the sea level air pressure (SLP) spectrum from Midway Is. (again, 1955 data) overlaid on the pressure spectrum from instrument PC. The great similarity of the energy levels and slopes strongly suggests (especially since the data are non-contemporaneous) a connection between the atmosphere and ocean bottom pressure at all frequencies under comparison. At periods greater than 1.5 days, strong coherence is found between bottom pressure and surface air pressure, as shown in the nearby poster by *Luther, Chave and Filloux*. However, no coherence has been found between bottom pressure and nearby surface or island air pressure at periods shorter than 1.5 days, despite the similarities evident in Figure 5. It is possible that this lack of coherence is due to the lack of high-quality, rapidly-sampled surface weather observations near the BEMPEX array. Note that the similarity of the spectra in Figure 5 does not arise from the isostatic adjustment of sea level to surface air pressure (the 'inverted barometer' effect) since this adjustment actually cancels the direct effect of air pressure below the sea surface.

Horizontal Coherence

FIGURE 6 exhibits the coherence function (amplitude and phase) between pressure records from instruments PF and PK. The stations are separated by 228 km and span the Mendocino Fracture Zone. Despite the distance and topography, the records are highly, significantly coherent at nearly all periods, even down to the Nyquist at 3.75 minutes. The relatively weak coherence at 17-18 hours occurs so close to the local inertial period (approximately 20 hours) that it is likely due to internal-inertial waves (the minimum coherence is not closer to a period of 20 hours due to spectral leakage from the highly coherent barotropic tides). Other relative minima in the coherence amplitude from 17 hours down to 4 hours may also be due to internal wave 'contamination'. The buoyancy period is approximately 4.5 hours. The relative maximum coherence amplitudes between 2 and 10 hours correspond to the overtidal peaks in Figure 3.

The coherence phase is near 0° at almost all periods greater than 1 hour, further suggesting the unimportance of baroclinic phenomena in these data. As period decreases from 1 hour, the phase in Figure 6 is seen to jump from near 0° to near 180° where it remains until a period of approximately 20 minutes at which point the phase jumps back to near 0°. These phases are indicative of standing oscillations. At short periods (less than 15 minutes) the coherence phase in Figure 6 monotonically increases as period decreases, consistent with the notion of waves propagating from PF to PK, where the waves have decreasing wavelength with decreasing period (as do surface gravity waves). [We have independently confirmed that the phase cycling is not due to an artificial, instrumentally-produced relative time lag between the records.]

Horizontally Standing Oscillations

For larger station separations, e.g., 593 km between PD and PF (**FIGURE 7**, where the abscissa has been expanded and the low frequencies truncated), the coherence amplitude remains significant out to small periods while the phase makes its first jump to 180° at a larger period than in Figure 6, and 6 distinct jumps from 0° to 180° or from 180° to 0° are evident compared to two jumps in Figure 6. Note also that the relative maxima in the coherence amplitude occur at periods centered in the bands of nearly constant phase, either 0° or 180° . For even larger separations, there are more phase jumps.

The phase jumps are more clearly seen if the phase is 'unwrapped'. Due to the behavior of the phase at the shortest periods, any jump in phase is considered a positive increase. Hence, **FIGURE 8** shows the 'unwrapped' phases from Figure 6, while the phases from the coherence between PD and PK (separated by 821 km; amplitudes not shown) unwrap as in **FIGURE 9**. The two phase jumps from 0° to 180° and back in Fig. 6 are clearly seen in Fig. 8. In Figure 9, 8 jumps are seen. (The smooth curves with λ labels are discussed later.)

This phase behavior, clustering around 0° or 180° , with more jumps at larger station separations and the first jump at a longer period for larger separations, is the behavior expected for a series of horizontally standing oscillations where the wavelength of the oscillations increases with period (as it does for surface gravity waves). That the ocean should support such high mode number oscillations is both remarkable and satisfying. Consider, for example, that at 30 minutes a surface gravity wave in a 5.6 km deep ocean has a wavelength of ~ 400 km, implying a nodal line roughly every 2° of latitude and 3° of longitude at 40°N ; thus scores of nodal lines exist across the Pacific.

Propagating Infragravity Waves

Figures 8 & 9 also more clearly exhibit the propagation of the short period infragravity waves. At periods shorter than 15 minutes, there is a strong suggestion that all the waves emanate from a single location, as can be shown with phase estimates based on the surface gravity wave dispersion relation,

$$\omega^2 = gk \tanh(kH) , \quad (1)$$

where g is the acceleration of gravity, k is the magnitude of the horizontal wavenumber, and H is ocean depth. Assuming plane wave propagation, the phase lag (in degrees) between two stations is given by

$$\phi(\omega) = \frac{360}{2\pi} D_0 k \cos(\lambda) , \quad (2)$$

where ω and k satisfy (1), D_0 is the distance between the stations, and λ is the acute angle defined by the direction of propagation of the waves and the line connecting the stations.

The phases defined by (2) are plotted in Figures 8 & 9 for two values of λ each. The distances D_0 and mean depths H between the stations are indicated on the plots. The good agreement between the observed phases and the theoretical phases at periods shorter than 15 minutes confirm that a single propagation direction (source) dominates this entire short-period band. Furthermore, the four pairs of BEMPEX stations with highest coherence amplitudes in this band yield directional estimates that put the source region at Vancouver Is., British Columbia, Canada. We are, of course, assuming that the band is dominated by infragravity waves generated by non-linear surface wave interactions at the coast, as recently demonstrated by *Webb et al.* [1991] in

the Atlantic.

Seasonal Variability

Energy density spectra of pressure from PK for three 18-day-long periods are superimposed in **FIGURE 10**. A strong seasonal dependence of the infragravity wave band is found. Additional spectra (not shown) indicate that this band has relatively high energy levels from October through April. During these months, the source region always appears to be in the vicinity of Vancouver Is. During the remaining months of the records, the source region is indeterminate due to weaker coherence amplitudes and more variable phase estimates in the infragravity wave band.

During the summer months, a rather narrow band peak within the infragravity wave band at approximately 6 minutes period is found (**FIGURE 11**). The source of this peak is indeterminate with the present dataset, but is likely to be somewhere in the Southern Hemisphere.

The 15 minute to 2 hour band, that we have concluded is dominated by horizontal normal modes, exhibits an unanticipated lack of seasonal variability in Figure 10. The modes in this period band apparently define a rather stable background energy level upon which earthquake-generated gravity waves will be superimposed.

References

- Filloux, J.H., 1969: Bourdon tube deep sea tide gauges. In: *Tsunami in the Pacific Ocean*, W. M. Sams, Ed., East West Center Press, pp. 223-238.
- Filloux, J.H., 1970: Deep sea tide gauge with optical readout of Bourdon tube rotation. *Nature*, 226, 936-938.
- Filloux, J.H., 1980: Pressure fluctuations on the open ocean floor over a broad frequency range: New Program and early results. *J. Phys. Oceanogr.*, 10, 1959-1971.
- Webb, S.C., X. Zhang and W. Crawford, 1991: Infragravity waves in the deep ocean. *J. Geophys. Res.*, 96, 2723-2736.

FIGURE 1

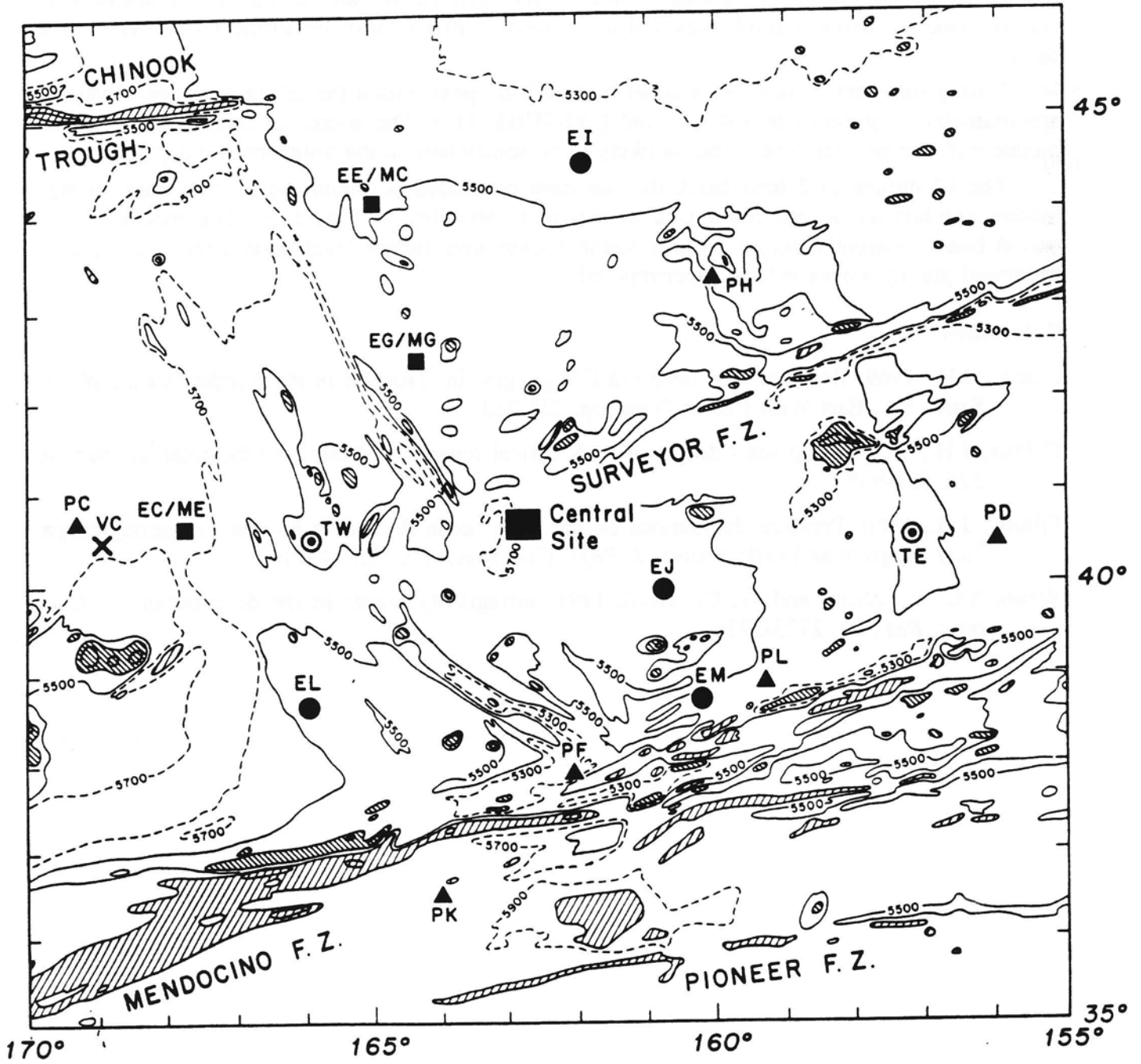


FIGURE 2

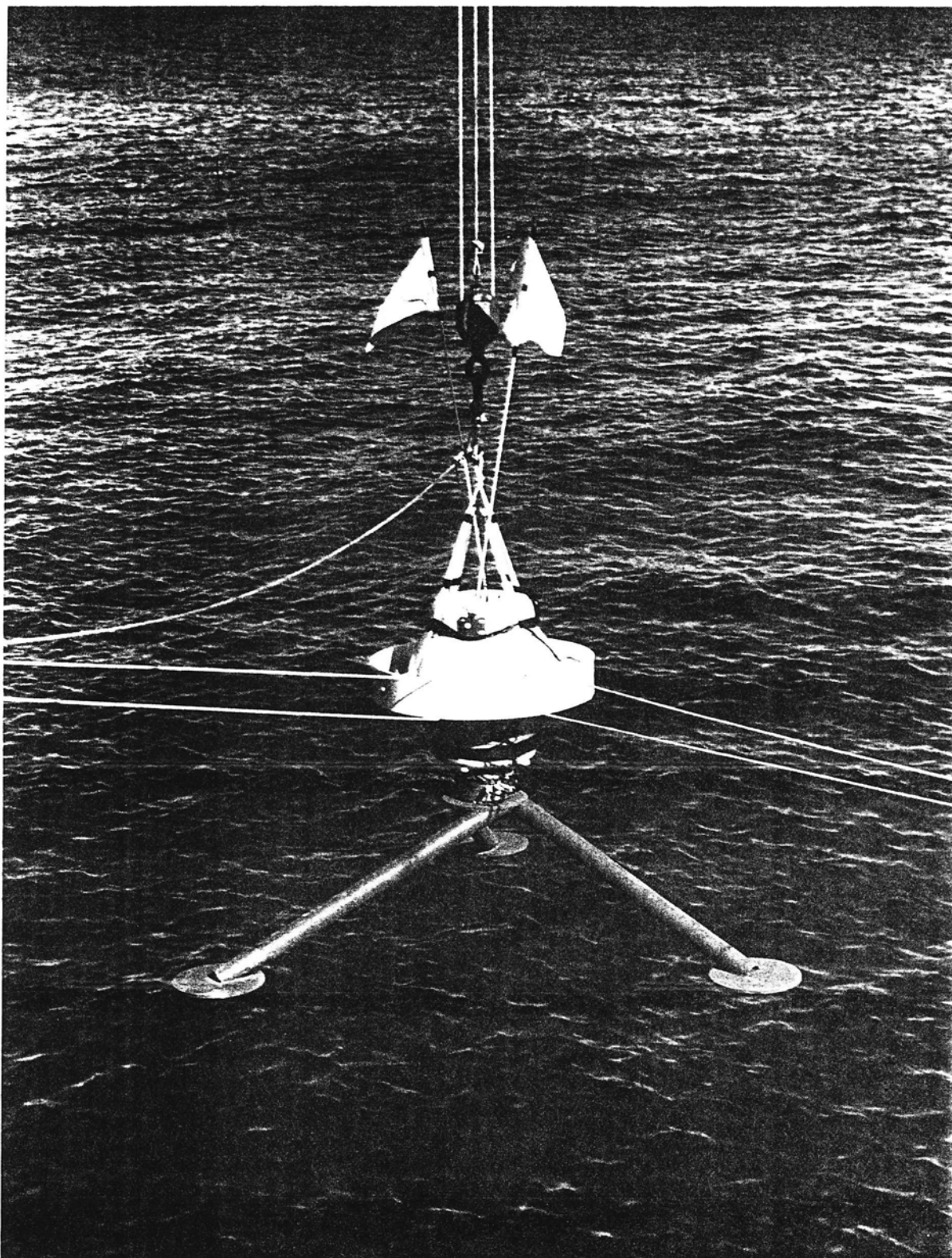
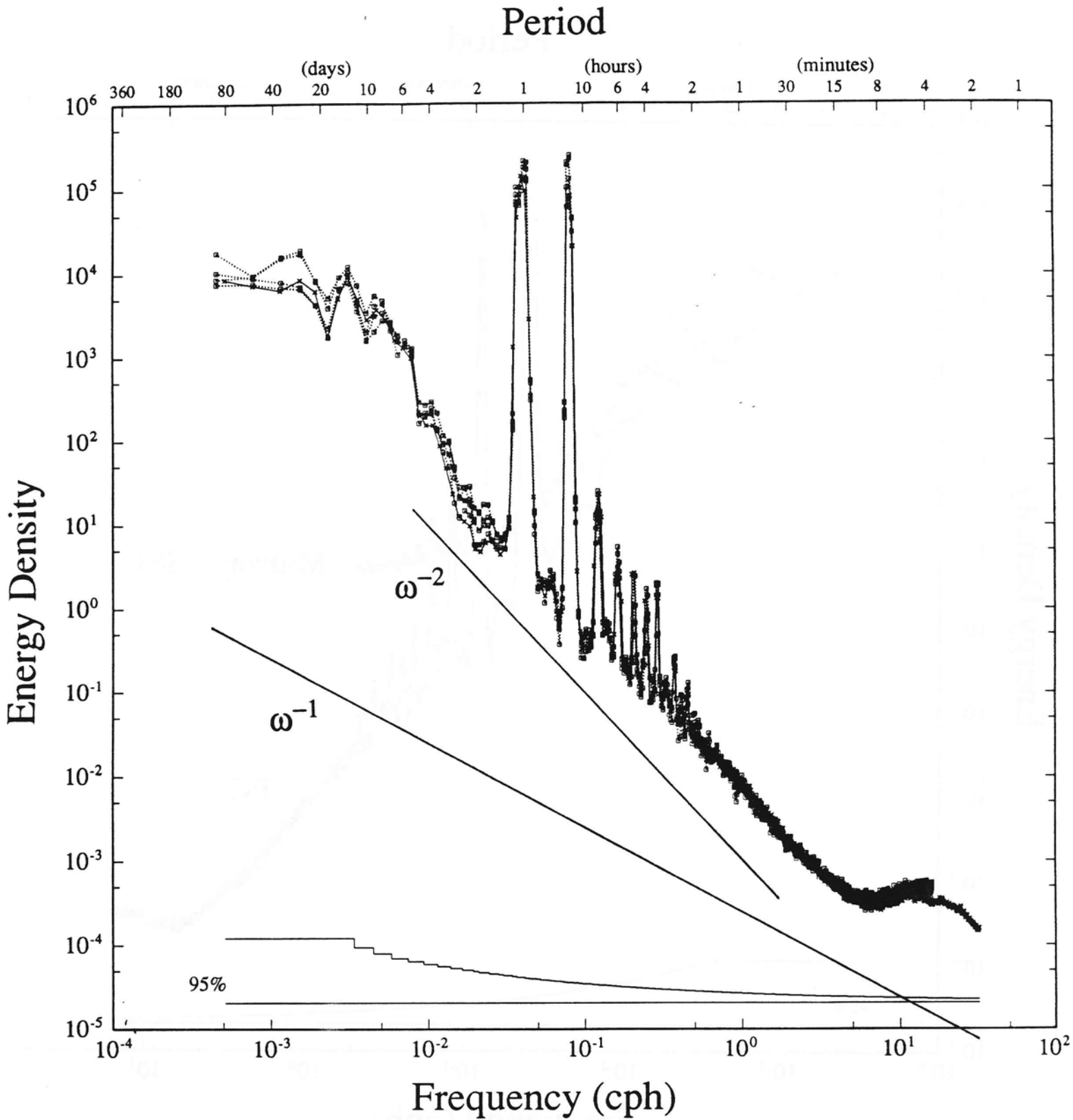


FIGURE 3



PC, PD, PF, PH, PK

FIGURE 4

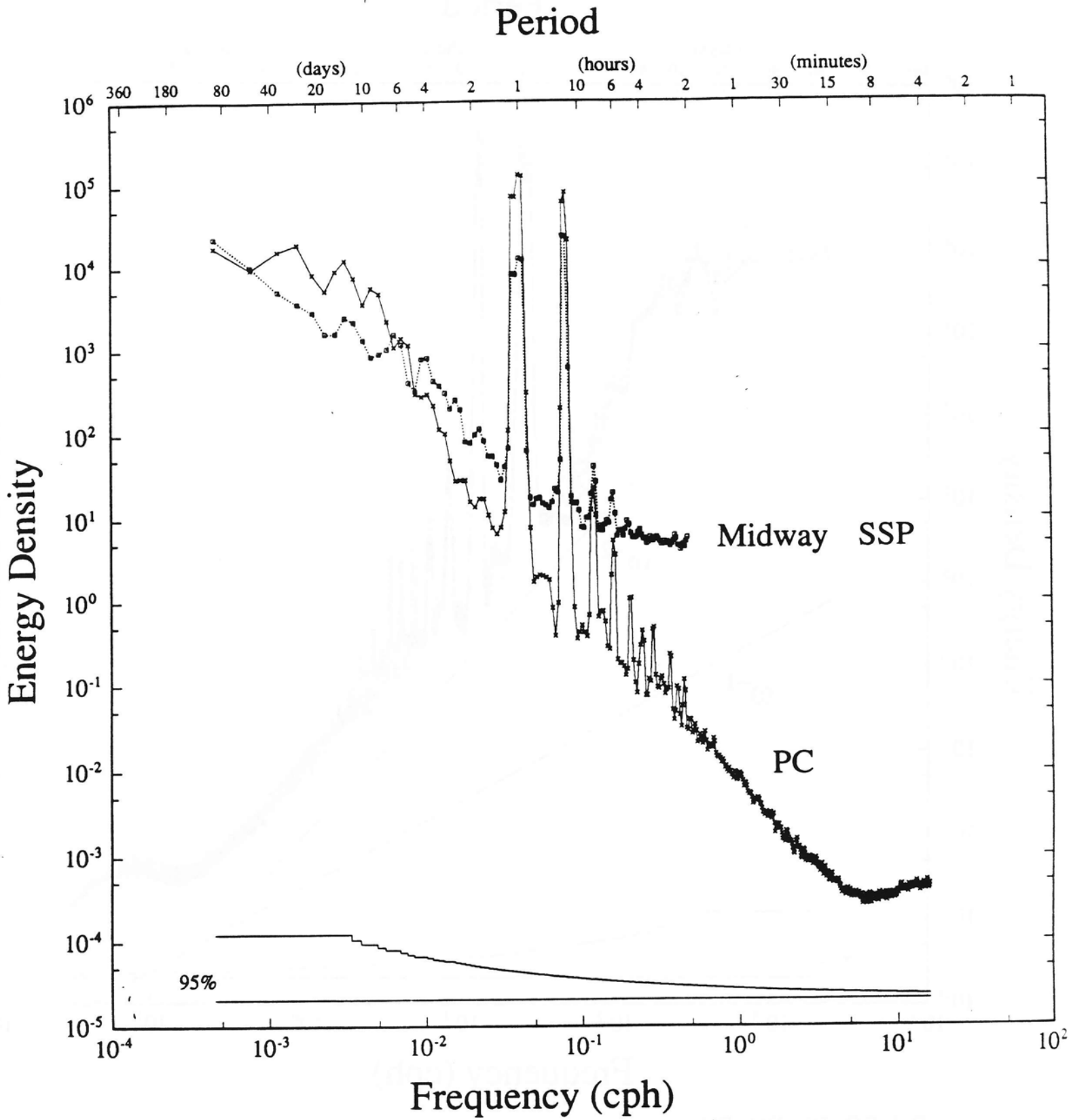


FIGURE 5

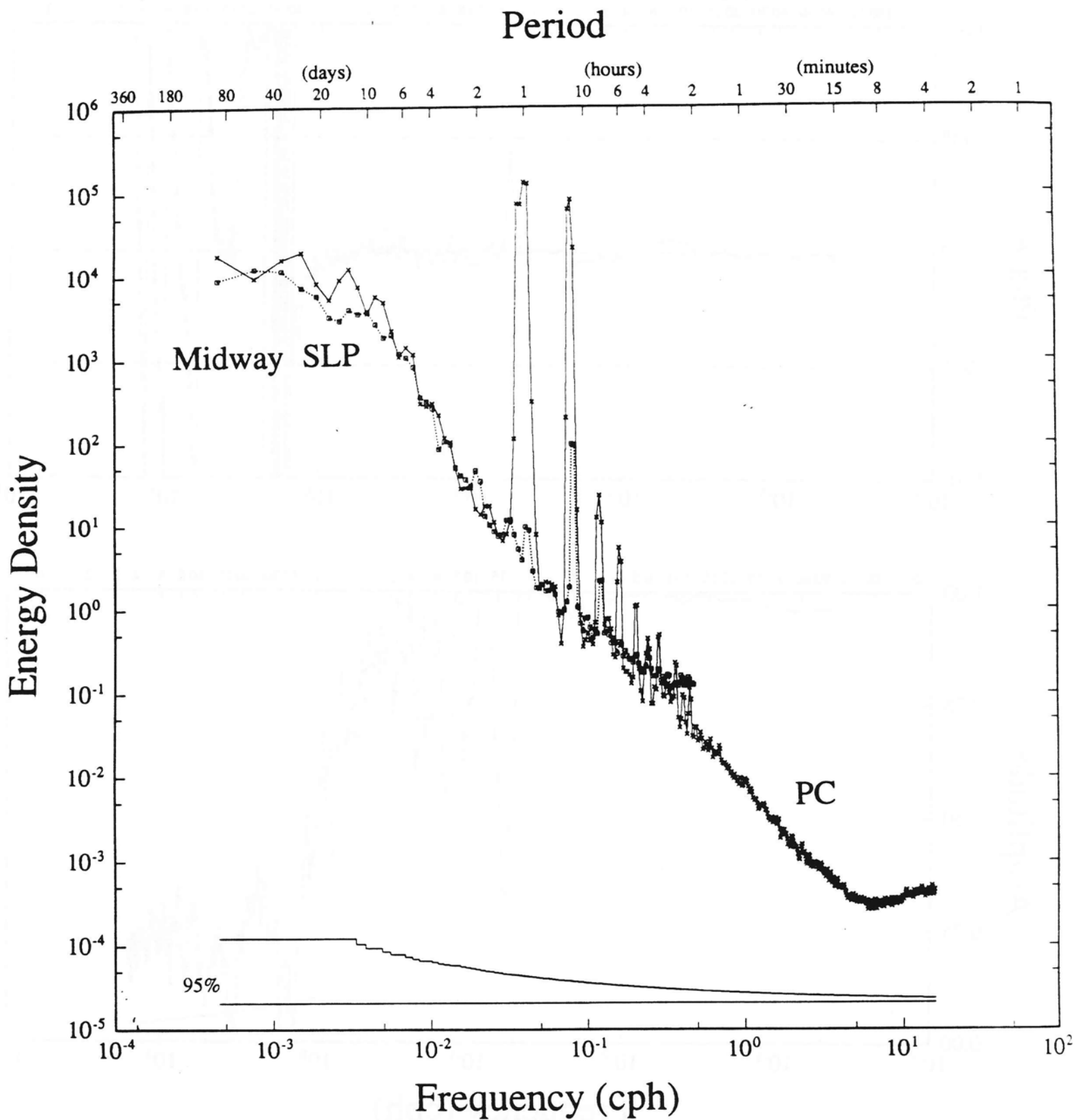
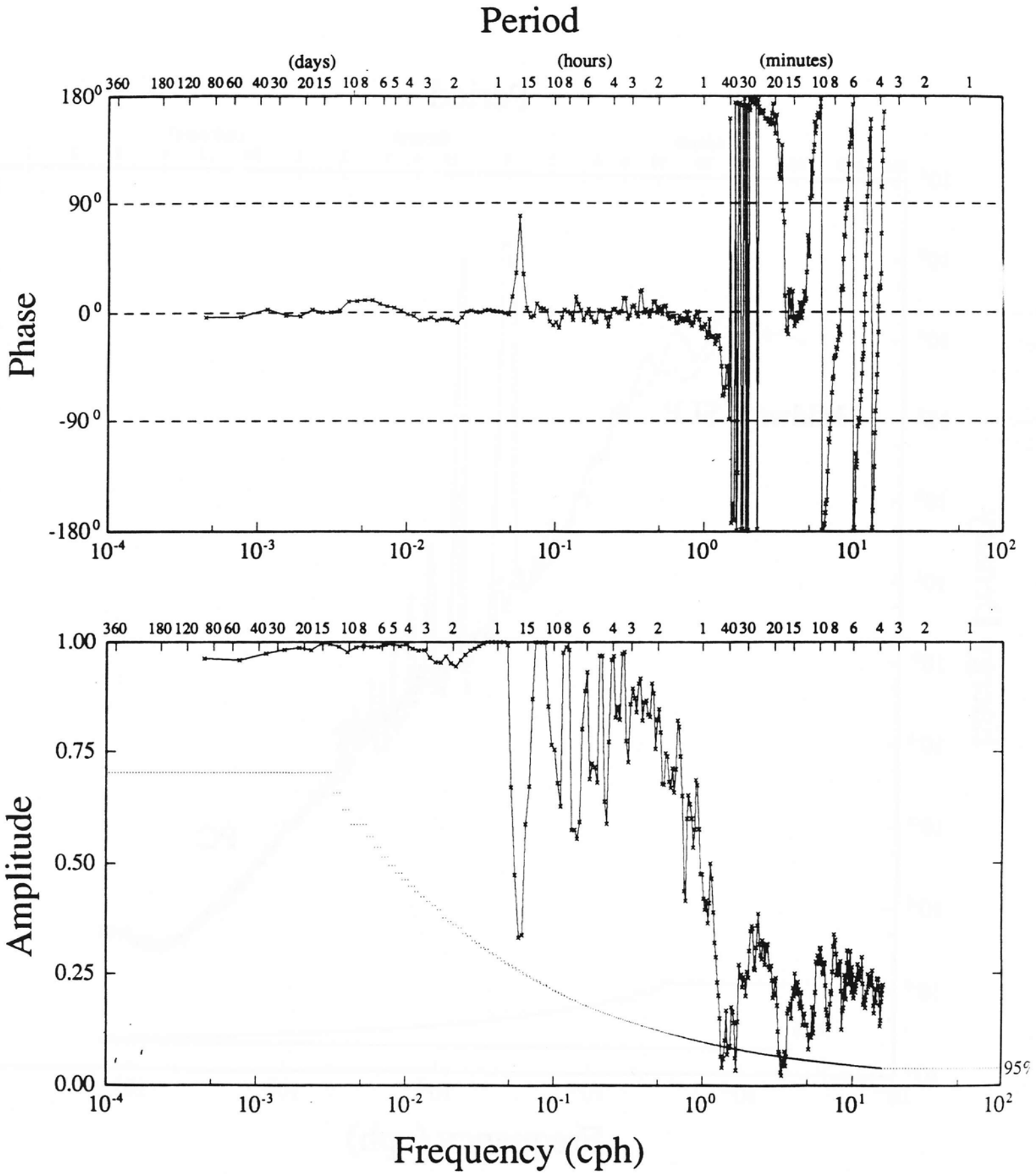
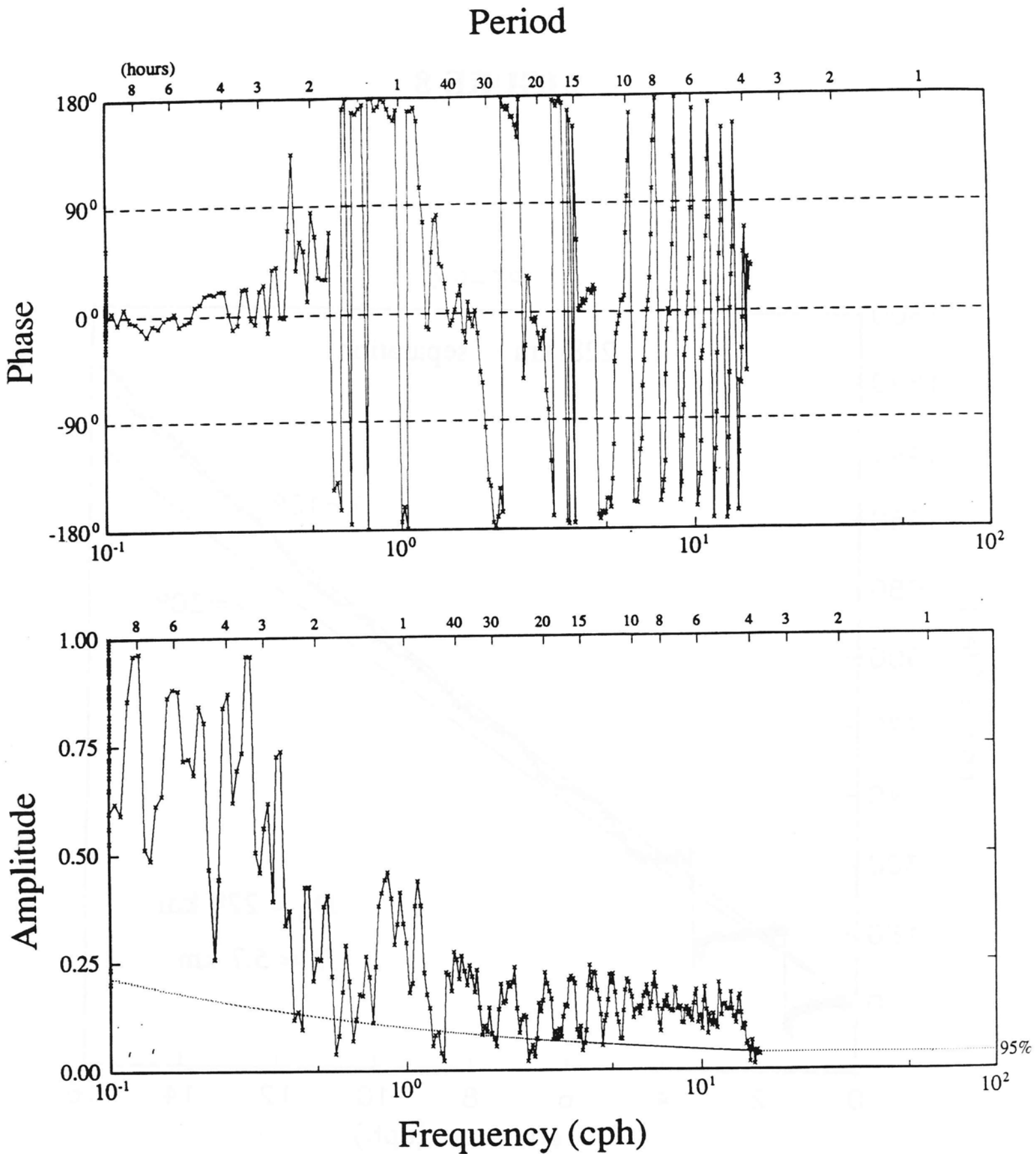


FIGURE 6



PF
PK 228 km separation

FIGURE 7



PD
PF 593 km separation

FIGURE 8

PF-PK

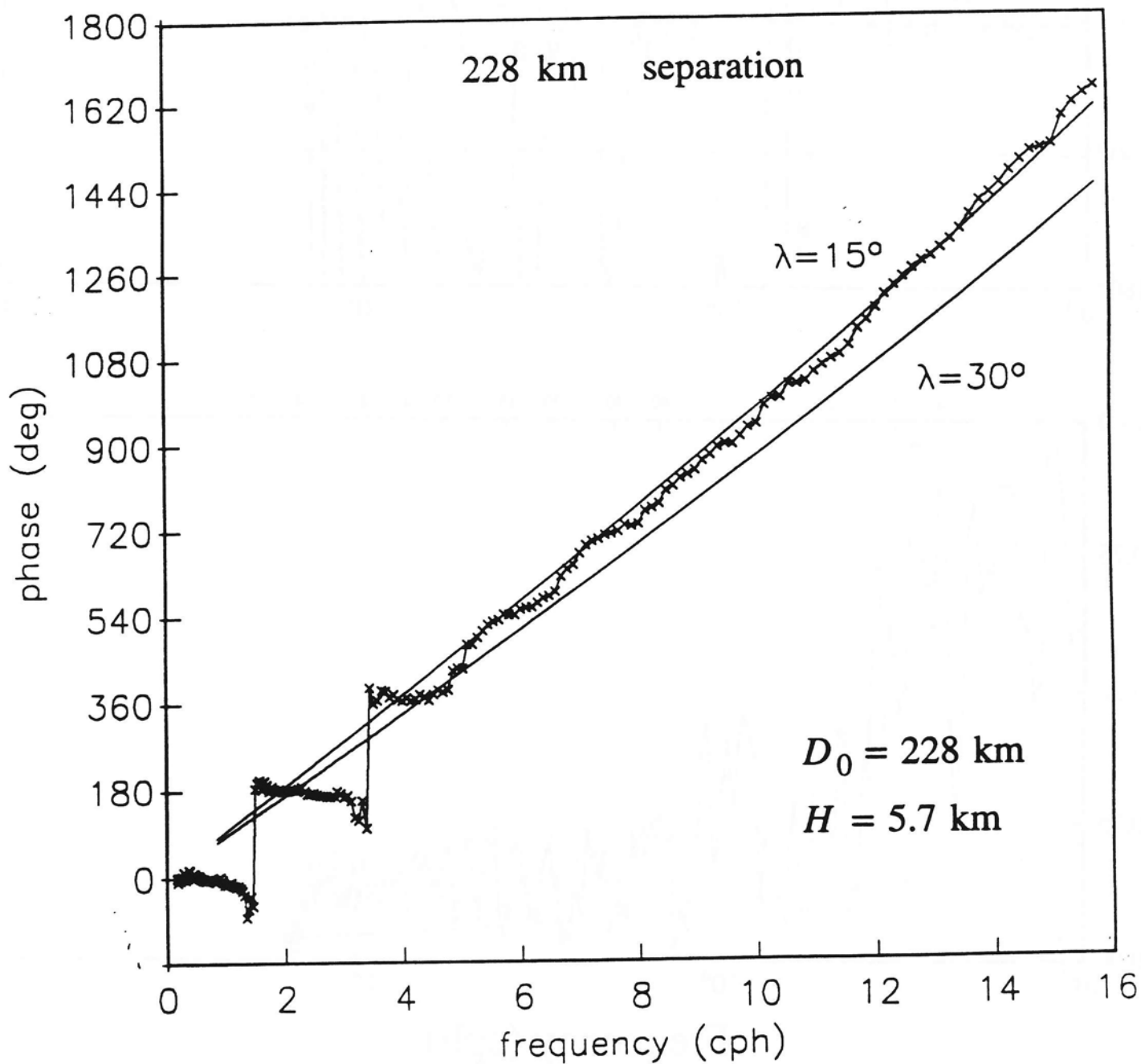


FIGURE 9

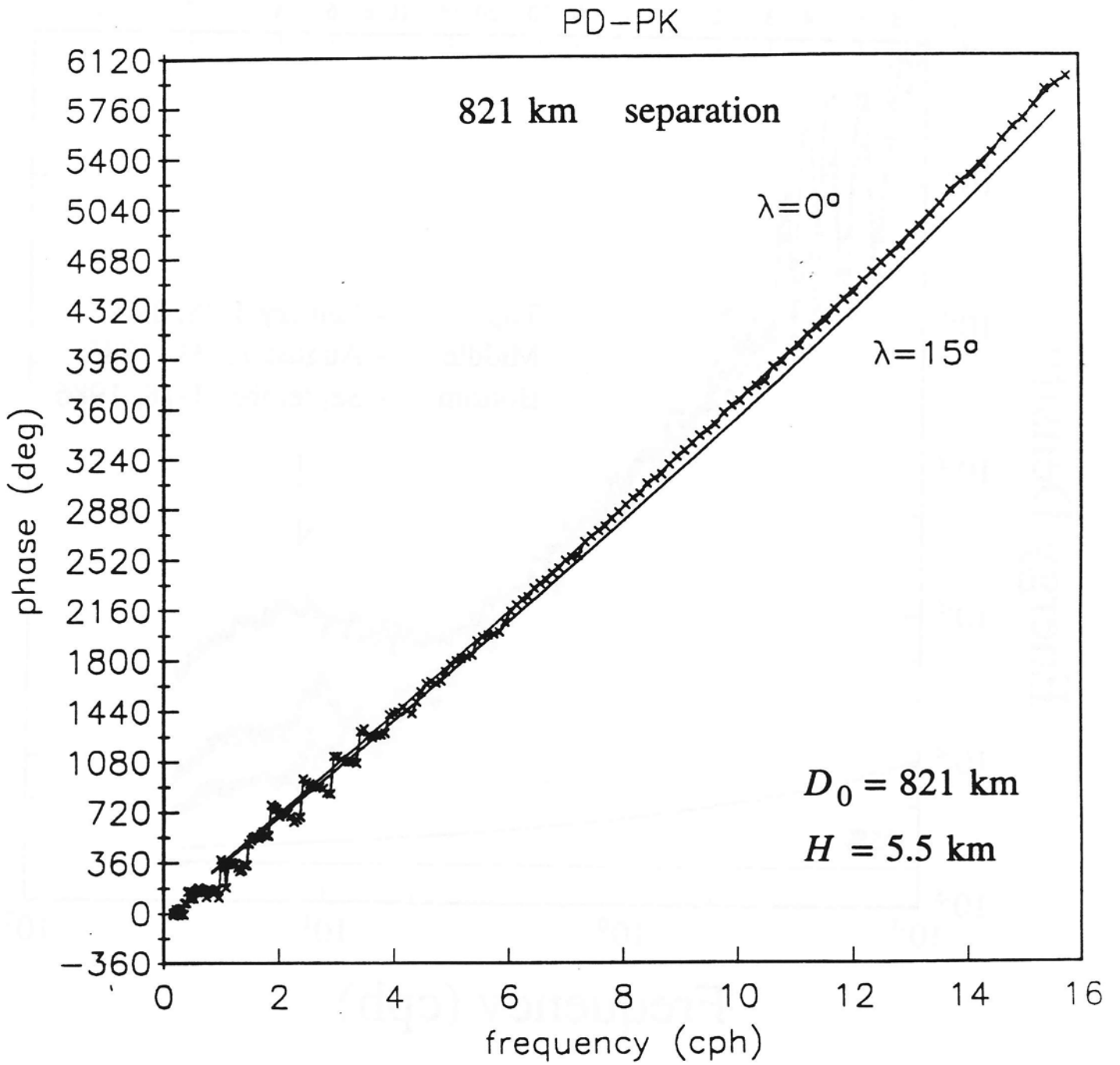
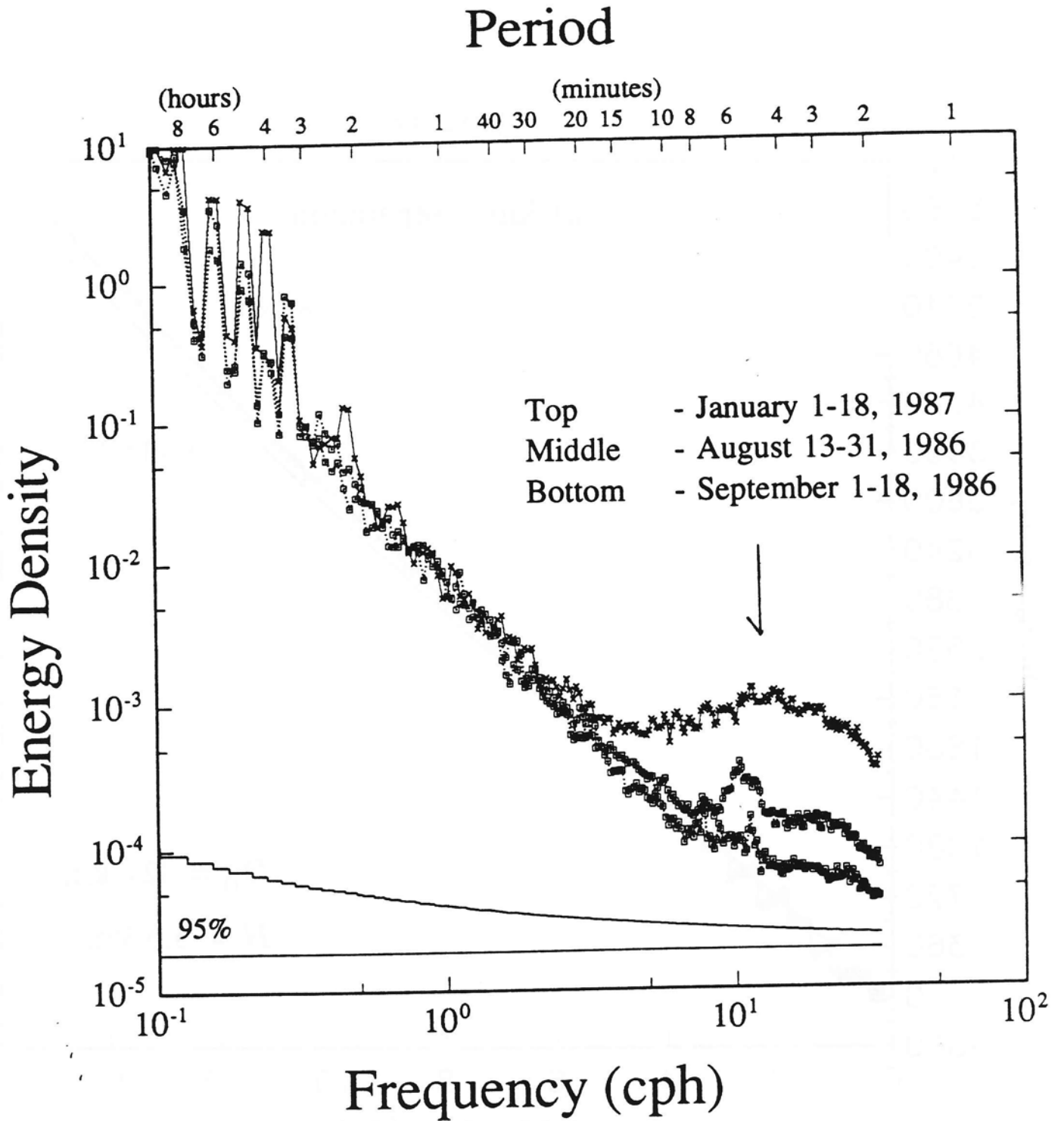
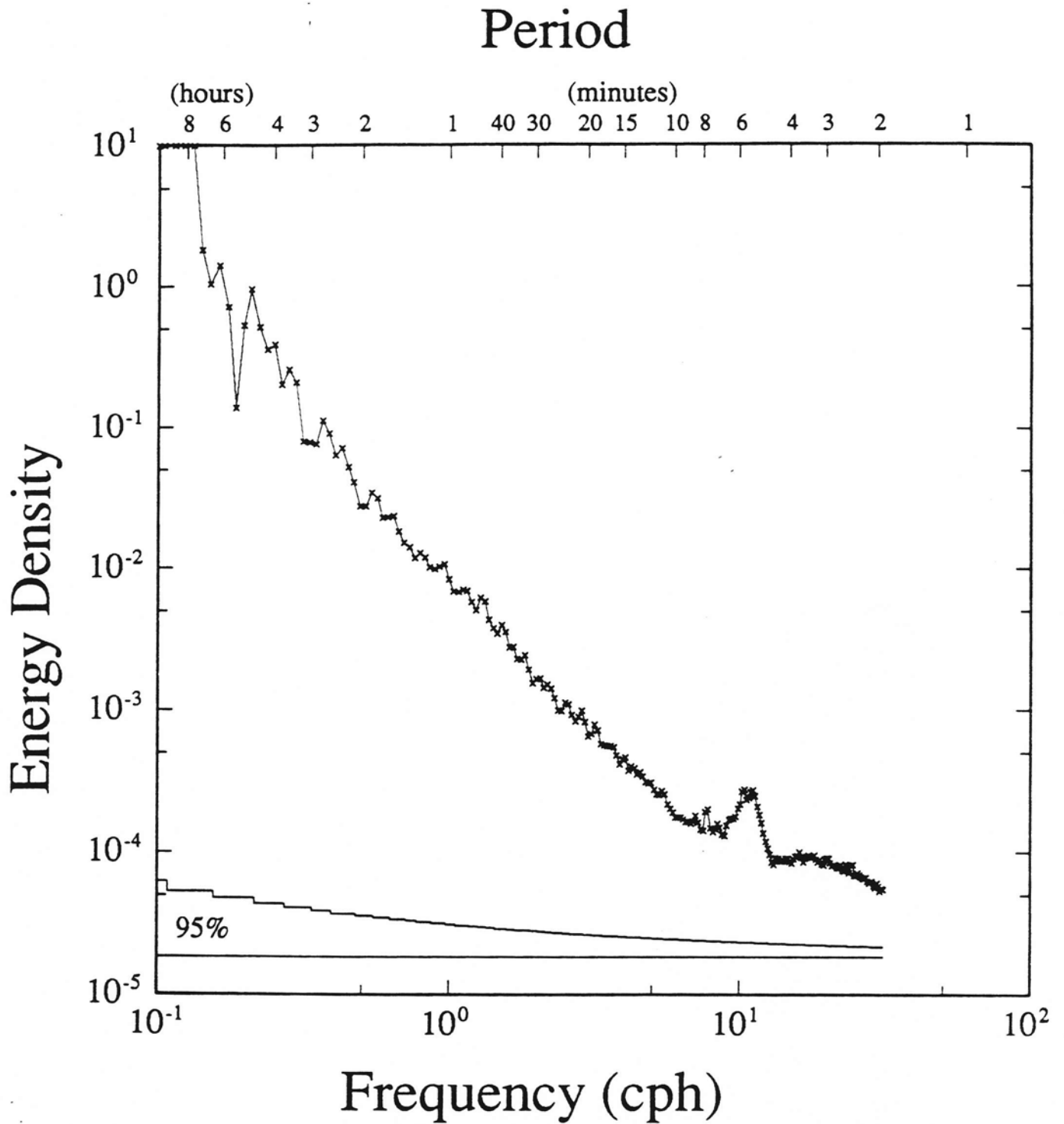


FIGURE 10



PK

FIGURE 11



PK

August 13-22, 1986 + June 4-30, 1987